

A Novel Framework for Segmentation of Stroke Lesions in Diffusion Weighted MRI Using Multiple b-Value Data

Shashank Mujumdar
Jayanthi Sivaswamy
IIIT-H, Hyderabad, India

R. Varma
KIMS Hospital
Hyderabad, India

L.T. Kishore
CARE Hospital
Hyderabad, India

Abstract

Diffusion Weighted MR Imaging (DWI) is routinely used for early detection of cerebral ischemic stroke. DWI with higher b-values ($b=2000$) provide improved sensitivity, higher conspicuity and reduced artifacts and thus improve the detectability of smallest infarcts than conventional DWI ($b=1000$). We propose a novel framework for accurately detecting stroke regions by combining information from multiple sources: $b2000$, $b1000$ data and the apparent diffusion coefficient map. The detected lesions are finally segmented using an active contour approach. The proposed method was tested on 41 datasets acquired with different protocols. A comparison of our method with a leading method [3] validates the effectiveness of our approach. The median dice coefficient, sensitivity and specificity for stroke segmentation were 0.84, 87.07% and 99.90% respectively. The strength of the proposed method is its ability to capture (and accurately segment) the small (and large) lesions in the data which are often missed by segmentation methods operating on a single b-value data.

1. Introduction

The use of Diffusion Weighted Magnetic Resonance Images (DWI) for identifying major ischemic change is popular due to their fast acquisition and increased sensitivity to acute ischemic stroke, relative to any other modality [2]. The contrast of the DWI scan at every voxel depends on the degree of diffusion of the water molecules in the voxel. Stroke lesions appear hyperintense on DWI and are inhomogeneous, with complex shapes and ambiguous boundaries with observed intensity variation [5] which makes manual segmentation difficult and time consuming. *Early* detection of regions of ischemic stroke (regardless of size and location) is critical for treatment. Automatic and accurate detection and segmentation of such ischemic stroke regions from DWI is the focus of the paper.

Prior methods for segmenting ischemic lesions in

DWI are of three types - manual, semi-automated and automated. Manual methods for segmentation may provide accurate results for further analysis but are labour intensive and operator-dependant [5]. Semi-automated methods rely on operator intervention in tuning the algorithm parameters or to initialize the algorithm. An example is the method in [8]. The proposed hybrid method combines the intensity-based information obtained statistically and the shape-based information obtained using the deformable active contour model to segment and measure the infarct volume. The snake contours are manually initialized.

Automated methods have received more attention recently. An artificial neural network is trained in [1] with multiple MRI sequences to predict the outcome of the ischemic stroke. A non-parametric density estimation technique is used in [6] for cerebral infarct segmentation followed by a refinement of the class boundaries using an edge confidence map. Identification of stroke slices, hemisphere and segmentation of stroke regions is achieved in [3] with a divergence measure based on the ratio of intensity probability density functions. Existing methods generally fail on low resolution and noisy data, particularly for the small-sized lesions.

The measured signal strength at a voxel in a DWI scan is quantified by the diffusion sensitivity b . The b-value is a control parameter which is fixed for every scan. The apparent diffusion coefficients (ADC) are derived using DWI from multiple b-values. ADC quantifies the diffusion process regardless of the shine-through artifacts. Imaging with higher b-value in a 1.5 Tesla scanner has been shown to improve the conspicuity, particularly for small-sized lesions and reduce number of shine-through artifacts, however, at the cost of SNR degradation and accompanied by accentuated anisotropic effects in regions where white matter tracts are prominent [5]. However, the automated methods for stroke detection to date, have been assessed only on $b1000$ data. We argue that a better strategy for accurate stroke detection and segmentation would be to

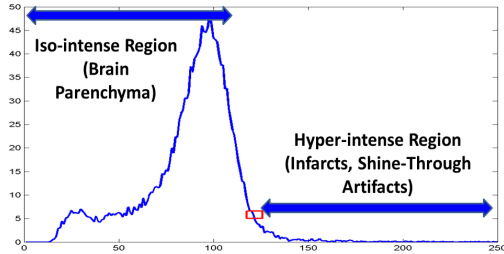


Figure 1. Regions shown on histogram of a DWI brain volume with background suppressed. Knee-point shown in red.

use information from scans acquired with low and high b-values. We have investigated this idea and propose a novel framework for combining information from b1000, b2000 scans for stroke detection and segmentation. The ADC map is generated using the Stejskal-Tanner equations: $ADC = \frac{-1}{b} \ln(\frac{S}{S_0})$, where S_0 is the signal intensity obtained with $b=0$ s/mm^2 and S is the signal intensity with $b \neq 0$ [7]. We utilise the ADC map to refine the detection and the segmentation results.

2. Proposed Method

Our objective is to accurately detect and segment the stroke lesions. The b2000 data with high sensitivity for stroke is suitable for finding candidate locations, however, will have high number of false positive locations (FP) due to reduced SNR. The b1000 (with low anisotropy effects) and the ADC (impervious to shine-through artifacts) are appropriate to help reject these FPs. An automatic windowing approach is proposed for pre-processing the b2000 data to suppress the noise and improve the local contrast and definition of the lesions. An extended version of the Chan-Vese [4] formulation of active contours is proposed for final segmentation.

2.1 Candidate Selection

At an early stage, stroke volume is much smaller than the brain volume and the infarct appears brighter than the brain tissue. Thus, in a DWI volume histogram (H_v), obtained after suppressing the non-brain-tissue region, the pixels belonging to lesion and shine-through artifacts will give rise to short peaks at the higher end as shown in Fig 1. Hence, a simple threshold set at the knee-point after the global maximum in H_v can help select the desired candidates. It is possible to employ a non-linear transformation to find this knee-point accurately, however, a rough method will suffice.

Candidate Refinement: In order to reject false candidates we first rely on the fact that the anisotropy effects increase with the b-value. Thus, while a true lesion appears bright and has a high local contrast (LC) on both b1000 and b2000 data, the false ones will have different

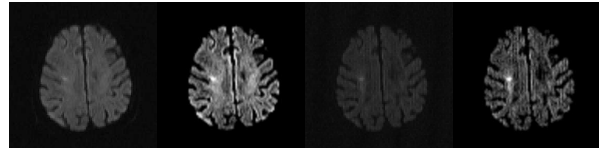


Figure 2. Results of windowing: (a) original b1000 (b) windowed b1000 (c) original b2000 (d) windowed b2000.

LC in these data. Hence, the ratio of the LC in these two data can serve as a good metric to detect false positives.

In order to compute the LC, a bounding box with a 3 pixel margin around every lesion is defined and the LC of the lesion is computed as $LC = \frac{|\mu_c - \mu_b|}{|\mu_c + \mu_b|}$ where, μ_c is mean of the lesion and μ_b is the mean of its local background. The normal background pixels are found by imposing a constraint on the ADC values. ADC of normal tissue pixels are expected to be within $[0.6 - 1.15] \times 10^{-3} mm^2/s$ according to [7]. The ratio of the LCs (b1000:b2000) was thresholded to reject the FPs. This threshold was empirically determined to be 0.6.

The above LC ratio-based rejection will not be able to reject FPs that arise due to shine-through artifacts. Hence, a second stage of rejection is needed. The ADC data is a good choice for this as mentioned earlier. The expected range for ADC values for stroke pixels is $[0.14 - 0.6] \times 10^{-3} mm^2/s$ [7]. Hence, the ADC value of every candidate is checked and all outliers are rejected. After this refinement stage we have a set of potential lesion locations which is passed on to the next stage for lesion segmentation.

2.2 Lesion Segmentation

Stroke lesions appear bright in DWI but are inhomogenous (within and across lesions) with complex shapes. Hence, detection of candidate pixels is a relatively easy task compared to *accurate* segmentation. An enhancement of the local contrast of the lesions is therefore a solution to improving the lesion definition. We propose an automatic windowing-based enhancement which is described next.

Automatic Windowing: The goal is to find the window setting that maximizes the local contrast for the lesions in a given dataset. For every given candidate, the LC is measured for a set of window parameters. The desired *best* window is the one which yields maximum LC for the lesions. Sample results of windowing are as shown in Fig 2. The lesions after applying the windowing operation are passed on to the segmentation stage.

Level Set Based Segmentation: Since the shape and size of the lesions vary widely an active contour based approach is appropriate for segmentation. We chose the

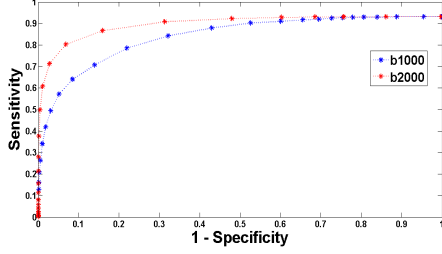


Figure 3. ROC plot for detection of small-sized lesions on b1000 vs b2000.

Chan-Vese model for active contours [4] which is an energy minimization framework based on the Mumford-Shah functional, solved using the level-set method. The objective of the Chan-Vese algorithm is to minimize the energy functional $F(c1, c2, C)$, defined by,

$$F(c1, c2, C) = \mu \cdot \text{Length}(C) + \nu \cdot \text{Area}(\omega) + \lambda_1 \int_{\omega} |u_0(x, y) - c1|^2 dx dy + \lambda_2 \int_{\Omega \setminus \omega} |u_0(x, y) - c2|^2 dx dy$$

where, $\mu \geq 0, \nu \geq 0, \lambda_1, \lambda_2 > 0$ are tuning parameters, Ω is a bounded set in \mathbb{R}^2 , C is an evolving curve in Ω , $u_0 : \bar{\Omega} \rightarrow \mathbb{R}$ is given image and $\omega \subset \Omega$. The constants $c1, c2$ dependent on C are the averages of u_0 inside C and outside C respectively. The first two (curvature) terms on the right hand side, enforce a smoothing constraint on the curve C while the next two (fitting) terms influence the evolution of the curve.

The above model was applied in our problem with a key difference. The pixel value, instead of being a scalar u_0 , is a vector with the b2000 and ADC values being the vector elements. Accordingly, the above equation is modified as

$$\hat{F}(c1, c2, c3, c4, C) = \mu \cdot \text{Length}(C) + \nu \cdot \text{Area}(\omega) + \lambda_1 \int_{\omega} |u_d(x, y) - c1|^2 dx dy + \lambda_2 \int_{\Omega \setminus \omega} |u_d(x, y) - c2|^2 dx dy + \lambda_3 \int_{\omega} |u_a(x, y) - c3|^2 dx dy + \lambda_4 \int_{\Omega \setminus \omega} |u_a(x, y) - c4|^2 dx dy$$

where, $\mu, \nu, \lambda_1, \lambda_2, \omega, \Omega, C$ are as defined in equation (1), $\lambda_3, \lambda_4 > 0$ are tuning parameters, $u_d : \bar{\Omega} \rightarrow \mathbb{R}$ is the b2000 DWI image and $u_a : \bar{\Omega} \rightarrow \mathbb{R}$ is the corresponding ADC map. The constants ($c1, c3$) and ($c2, c4$) dependent on C are the averages of (u_d, u_a) inside C and outside C respectively. We fix $\lambda_1 = \lambda_2 = \lambda_3 = \lambda_4 = 1$ and $\nu = 0$ and the segmentation is the minimization of the energy functional $\hat{F}(c1, c2, c3, c4, C)$.

Since the active contour based approach can lead to erroneous boundaries for small-sized lesions ($< 1\%$ of image size), an ADC-based post-processing of the small-sized segmented results is done as described in Section 2.1.

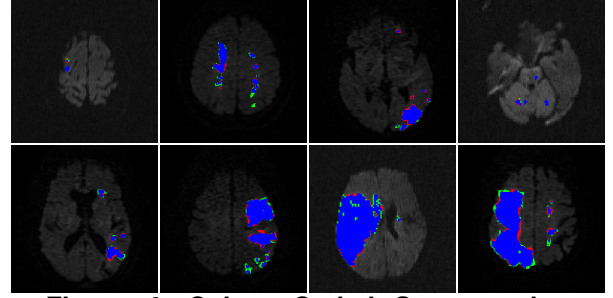


Figure 4. Colour Coded Segmentation Results shown overlaid on b2000 data, Blue:TP, Red:FP and Green:FN.

3. Experiments and Results

Data: 41 DWI volumes of confirmed stroke patients were collected from two local hospitals which had different types of scanners and used different methods of data acquisition. The different b-value data were acquired sequentially in Scanner-1 and simultaneously in Scanner-2. The ADC maps from Scanner-1 were independently generated for both the b1000 and b2000 data using the Stejskal-Tanner equations [7]. Expert markings of lesions were also collected for all the 41 volumes to serve as ground truth (GT). The full data description is provided in Table 1.

Table 1. Data Description.

Scanner	Data Sets	Acquired Data	Voxel Size	Matrix Size (MS) Pixel Depth (PD)
Scanner-1	29	b=0, b=1000, b=2000,(Sequential), ADC=Post Acquisition	0.98×0.98×6.32mm	MS = 256×256×22 PD = 16 bits
Scanner-2	12	b=0, b=1000, b=2000,(Simultaneous), ADC = In Acquisition	1.95×1.95×7.28mm	MS = 128×128×20 PD = 12 bits

The first experiment is aimed at determining the effectiveness of the b2000 data in the detection stage. Detection of smallest early ischemic changes are proven to be better in b2000 over b1000 [5]. The sensitivity vs. specificity curves were generated for detection of small lesions ($< 1\%$ image size) by varying the knee-point described in Section 2.1. The obtained plot is shown in Fig 3 which agrees with [5].

Next, the segmentation performance was assessed and compared with a leading method [3]. For the segmented results, true-positives (TP), false-positives (FP), false-negatives (FN) and true-negatives (TN) were determined. Sample colour coded segmented results are shown in Fig 4. The colour code is as follows: blue, red and green pixels indicate TP, FP and FN pixels, respectively. Dominant blue pixels indicate the robustness of the algorithm in accurately capturing different-sized lesions in the data. The Dice coefficient (DC) [9] measures the spatial overlap between the GT and the results of segmentation. A value of zero indicates no overlap,

Table 2. Descriptive Statistics & Evaluation Metrics.

Statistics	Maximum	Minimum	Mean	Median	Std	CV
Sensitivity (%)	97.30	43.75	83.68	87.07	10.58	0.1264
Specificity (%)	99.99	99.01	99.79	99.90	0.25	0.0025
DC	0.96	0.41	0.81	0.84	0.12	0.1530
$DC = 2 * \frac{A \cap G}{A \cup G}$ $SN = \frac{TP}{TP+FN}$ $SP = \frac{TN}{FP+TN}$						

while a value of one represents a perfect overlap. The sensitivity (SN) and specificity (SP) figures were also calculated. The statistics of DC, SN and SP are presented in Table 2. In DC calculation, A is the segmented volume by the algorithm and G is the ground truth. The coefficient of variation (CV) reported here is the ratio of the standard deviation (Std) and the mean values. Ideal value of CV is 0 and DC is 1. These are reported to observe the trend in the results.

Our dataset contained 324 large-sized lesions and 286 small-sized lesions. In light of this fact, the high median values of SN, SP and DC with corresponding low CV values indicate that the segmentation algorithm is robust to size and shape variations in lesions. The datasets were acquired from two different scanners with different acquisition protocols and the algorithm appears to be robust to these factors.

An experiment was also done to study the degree of improvement in the segmentation accuracy (at the boundaries) due to b2000 data. The segmentation was performed on b1000 and b2000 data separately, for only true lesion locations (found from GT), for all the volumes. The median DC values for the segmentation results were 0.68 and 0.83 for b1000 and b2000 data respectively. Thus, an improvement of 22.06% in the segmentation accuracy was observed on b2000 data.

While the experiment results indicate the merit in using b2000 data for accurate segmentation it does not indicate the role, b1000 and ADC can play, in detecting the lesion locations in the first place. Hence, a final experiment studied the effectiveness of the complete pipeline by comparing the proposed algorithm with a leading method [3]. The results are presented in table 3.

The method in [3] captured significant sized lesions, but completely failed in capturing the small sized lesions. This results in a lowered DC value. While both the methods have high SP, our method has significantly improved SN. This indicates that inclusion of b1000 and ADC is aiding the improvement in performance.

4 Discussion & Conclusions

A novel technique for segmentation of stroke lesions in brain DWI data using multiple b-values (b1000 & b2000) and the ADC maps is presented. The method is robust to data acquired on multiple scanners with dif-

ferent acquisition processes. The qualitative and quantitative results reported in the study show superiority of the method in accurately detecting and segmenting the stroke lesions over the conventional methods operating only on the b1000 data. The median DC, sensitivity and specificity for stroke segmentation were 0.84, 87.07% and 99.90% respectively. The method is automated and therefore could assist the clinicians in diagnosis.

Table 3. Comparison with [3] method.

Method	Median SN (%)	Median SP (%)	Median DC
Our Method	87.07	99.90	0.84
[3] method	56.40	99.30	0.60

The improvement in performance of the proposed method comes at the expense of computational cost due to the need to process additional data. However, in stroke cases where there are only small-sized lesions, the gain to be obtained in correctly detecting (and segmenting) the presence of the lesion can outweigh the additional computational burden.

5 Acknowledgement

We acknowledge the collaboration between GE Global Research, Bangalore, India and IIT-Hyderabad, India which facilitated development of the work described in this study.

References

- [1] H. Bagher-Ebadian et al. Predicting final extent of ischemic infarction using artificial neural network analysis of multi-parametric mri in patients with stroke. *PLoS one*, 6(8):e22626, 2011.
- [2] P. Barber et al. Identification of major ischemic change: diffusion-weighted imaging versus computed tomography. *Stroke*, 30(10):2059–2065, 1999.
- [3] K. Bhanu Prakash et al. Automatic processing of diffusion-weighted ischemic stroke images based on divergence measures. *CARS*, 3(6):559–570, 2008.
- [4] T. Chan and L. Vese. Active contours without edges. *TIP*, 10(2):266–277, 2001.
- [5] H. Kim et al. High-b-value diffusion-weighted mr imaging of hyperacute ischemic stroke at 1.5 t. *AJNR*, 26(2):208–215, 2005.
- [6] N. Montiel et al. Robust nonparametric segmentation of infarct lesion from diffusion-weighted mr images. *EMBS*, pages 2102–2105, 2007.
- [7] R. Sener. Diffusion mri: apparent diffusion coefficient (adc) values in the normal brain and a classification of brain disorders based on adc values. *CMIG*, 25(4):299–326, 2001.
- [8] B. Stein et al. Statistical and deformable model approaches to the segmentation of mr imagery and volume estimation of stroke lesions. *MICCAI*, pages 829–836, 2001.
- [9] K. Zou et al. Statistical validation of image segmentation quality based on a spatial overlap index. *Academic Radiology*, 11(2):178–189, 2004.